2018-07-21

Process-property-performance relationships in CFRP composites using fractal dimension

Mahmood, A

http://hdl.handle.net/10026.1/11868

10.1088/1757-899X/388/1/012013
IOP Conference Series: Materials Science and Engineering
IOP Publishing

Process-property-performance relationships in CFRP composites using fractal dimension

To cite this article: Amjed Saleh Mahmood *et al* 2018 *IOP Conf. Ser.: Mater. Sci. Eng.* **388** 012013

IOP Conf. Series: Materials Science and Engineering **388** (2018) 012013 doi:10.1088/1757-899X/388/1/012013

Process-property-performance relationships in CFRP composites using fractal dimension

Amjed Saleh Mahmood [1, 2], M Neil James [1, 3] and John Summerscales [1]

[1]Advanced Composites Manufacturing Centre, School of Marine Science and Engineering, Reynolds Building, University of Plymouth, Plymouth PL4 8AA, England

[2]Head of Electromechanical Engineering Department, College of Engineering, Samarra University, Samarra, Iraq

[3]Department of Mechanical Engineering, Nelson Mandela Metropolitan University, Summerstrand Campus (North), Port Elizabeth, 6031, South Africa

E-mail: dramjed78@gmail.com

Abstract. The present study considers the dependence of the mechanical properties on the fibre architecture for composite laminates. Woven carbon/epoxy fabric composites were manufactured by the resin transfer moulding (RTM) process. Image analysis and fractal dimension (D) were used to quantify fibre distribution and resin-rich volumes (RRV) then correlate these data with the mechanical properties of the fibre-reinforced composites. The static strength of these composite laminates showed a clear dependence on the fibre distribution. Four-point flexural fatigue tests were conducted under load control, at a sinusoidal frequency of 10 Hz under load amplitude control with a stress ratio (R=σmin/σmax) of 0.1. Specimens were subjected to maximum fatigue stresses of 95% to 82.5% step 2.5% of the ultimate flexural strength (UFS). The fatigue properties of the composite laminates are shown to have statistically significant correlations with the fibre distribution and the static properties of the laminates. A loss of 5-6 % in the flexural modulus of the composite laminates predicted an increasing probability of failure of the composite laminates under fatigue loading. This occurs at about 90% of the fatigue life at a particular stress level.

1. Introduction

The increasing demand for high performance materials, (i.e. those which have high modulus- and/or high strength-to-weight ratio combined with improved fatigue performance and high toughness) has led to rapid advances in the field of fibre–reinforced composites. The estimated global demand could reach 146,000 tonnes of carbon composites produced annually by 2020 across the various applications [1]. High-performance composites often use autoclave consolidation to improve their mechanical properties by increasing the fibre volume fraction, and hence reducing the defect population. However, autoclaves are both an expensive capital equipment cost and a significant constraint on the rate of production. There is therefore increasing interest in composite manufacturing processes which do not require an autoclave stage, e.g. the resin transfer moulding process (RTM). Whilst out-of autoclave (OOA) manufacturing can increase the production rate of composite components and significantly reduce the energy consumption, it can also lead to lower fibre volume fractions (Vf) due to the compressibility characteristics of the fibres [2-5]. The lower Vf, obtained at reduced consolidation pressure, may lead to resin-rich volumes (RRV) in the composite and a consequent disproportionate reduction in the mechanical properties of the composite laminates. The level of RRV is highest in spray-up and hand-lamination techniques (no consolidation pressure), less common in OOA and liquid composite moulding (LCM) procedures, and lowest in autoclave and compression moulding processes. Increasing the pressure during manufacturing reduces the RRV, especially during autoclave consolidation [6, 7]. The improved nesting of fibres leads to improved mechanical properties (both static and fatigue).

Studying the effect of fibre volume fraction on the performance of composite laminates, without taking full account of the effect of changes in the fibre architectures and the consequent RRV for the reinforcement system in use, may lead to erroneous estimates of the service performance. Fractal dimension (D) looks promising for the quantification of the fibre distribution. Researchers [8-25] have already used D to correlate some mechanical properties and processing parameters. One of the techniques used to calculate the fractal dimension is the box-counting method which has been widely used in D research [17, 26-33].

The mechanical properties of composites have been extensively considered in analytical and experimental investigations for over four decades for both static properties [34-45] and fatigue properties [46-57]. These studies indicate that the fibre distribution is the most common parameter that links other parameters such as the RRV and internal defects, the stacking sequence, the stiffness and the anisotropic properties of the composite laminates. Modelling and prediction of the fatigue life requires significant experimental S-N data for each type of composites [58-60]. This study is believed to be the first systematic endeavour reported in the literature aimed at correlating fractal dimension with the fatigue life for continuous woven reinforcement fabric laminates.

2. Experimental methodology

RTM is a process for producing composite laminates by clamping the reinforcement between the upper and lower parts of a mould tool, then infusing resin to fill the inter fibre porespace. A schematic of the RTM process is given in Figure 1. Two 6K carbon fibre fabric architectures were woven by Carr Reinforcements using the same batches of fibre for each warp and weft. The modulus of elasticity of the carbon fibres was 235 GPa. The areal densities of the two fabrics tested in this work were: plain weave 300 g/m^2 and twill weave 320 g/m^2. The resin was Sicomin SR8100 epoxy with Sicomin SD8824 hardener and a weight mix ratio of 100:22. Six different composite laminate plates were manufactured for this work, comprising:

- 3 plain weave plates, utilising either 4 layers, 5 layers or 6 layers of fabric.
- 3 twill weave plates, utilising either 4 layers, 5 layers or 6 layers of fabric.

Images of the microstructure were captured from polished sections using an Olympus BX60 microscope with Olympus Stream image analysis software (SM04733) and analysed using the ImageJ software package with the FracLac add-in.

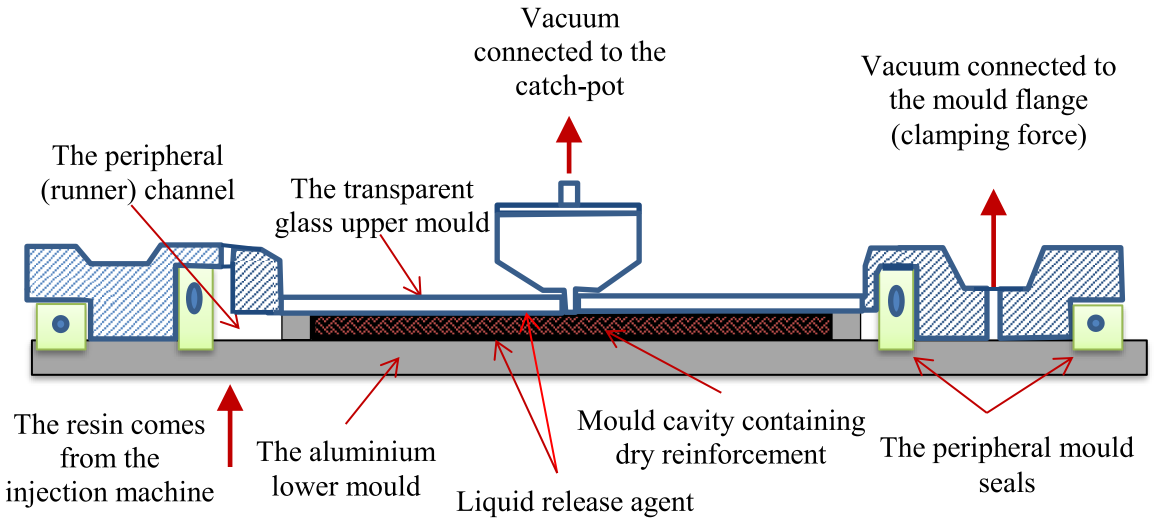

Figure 1: The RTM process as implemented in this study.

Four-point bend (static and fatigue) tests were conducted according to the British Standard EN ISO 14125:1998. An Instron Electropuls E300 (serial number: 5527-103) with a ±5 kN load cell (serial number: 107190) and test speed 1 mm/min was used. Tests were carried out in the warp and the weft direction with specimen dimensions of 100*15*2 mm (L*W*T). Five rectangular samples were cut in both the warp and weft directions from each of the six composite laminate plates: plain or twill and 4, 5 or 6 layers (giving 60 samples in total). The interlaminar shear strength was assessed in this work using the ISO 14130:1998. Five samples were cut from each direction of 3 different plates for each weave style (again giving 60 samples in total). Tests were conducted using an Instron 5582 universal testing machine (serial number: 5582J7466) with a ±100 kN load cell (serial number UK195) and a test speed of 1 mm/min. The four point sinusoidal bend S-N fatigue tests were performed with a stress ratio ($R=\sigma_{min}/\sigma_{max}$) of 0.1. The tests were carried out on specimens machined with their longitudinal axis parallel with either the warp or the weft directions in the as-manufactured laminate plates. The load amplitudes were chosen on the basis of using a set percentage of the ultimate flexural strength UFS.

3. Fractal dimension (D)

ImageJ with FracLac software creates an imaginary network of boxes over the binary image of the sampling region of the laminate. At every step i, the program counts the number of boxes that contain fibre. A ln-ln plot of number of fibre-containing boxes, against box size is produced as the output from this process. Each iteration gives a point in this plot. The slope of the regression line equals the negative estimated fractal dimension of the laminate. For different grid positions, the mean fractal dimension has been calculated. For consistent image analysis, all images should have (a) the same pixel size, (b) uniform assignment of colors to different parts of the microstructure (e.g. resin as black background), and (c) the ImageJ software options set to obtain the same size of sampling grid area in each case.

4. Results and discussion

Table 1 presents the mean mechanical properties for both fibre architectures (plain and twill weave) with 4, 5 and 6 layers of fabric. Figure 2 illustrates the correlation between UFS and D for all laminates, a strong second order correlation is apparent, with $R^2 = 0.9034$ and p=0.000027. Figure 3 illustrates the correlation between ILSS and microstructure, characterised by the fractal dimension. There is a reasonable correlation between the two parameters as $R^2 = 0.5579$ and p=0.025 as the ILSS is strongly influenced by resin properties and interfacial adhesion rather than depending solely on the fibre distribution. Figure 4 presents the correlation between E_f and microstructure, where $R^2 = 0.6822$ and p=0.005. From the data contained in Figures 2 to 4, the regression equations linking mechanical properties with fibre distribution via D were found to be:

$$UFS\ (MPa) = -21339D2 + 82155D - 78329 \tag{1}$$
$$ILSS\ (MPa) = -550D2 + 2131D - 2014 \tag{2}$$
$$E_f\ (GPa) = -1278D2 + 4881D - 4616 \tag{3}$$

Table 1 : The mean mechanical property and image analysis data for woven carbon fibre laminates.

Laminate	Direction	Notation	D	UFS(MPa)	ILSS(MPa)	E_f(GPa)
4 layers (Plain)	Warp	P4wp	1.835	561	43.8	38.9
	Weft	P4wt	1.809	463	40.5	31.2
4 layers (Twill)	Warp	T4wp	1.826	548	46.8	30.9
	Weft	T4wt	1.862	608	45.9	34.6
5 layers (Plain)	Warp	P5wp	1.859	670	47	40.8
	Weft	P5wt	1.841	567	44.1	39.2
5 layers (Twill)	Warp	T5wp	1.844	642	51.3	36.8
	Weft	T5wt	1.893	719	49.3	42.4
6 layers (Plain)	Warp	P6wp	1.892	725	48.9	45.6
	Weft	P6wt	1.850	623	44.9	41.4
6 layers (Twill)	Warp	T6wp	1.863	711	50.1	40.6
	Weft	T6wt	1.912	743	51.7	42.4

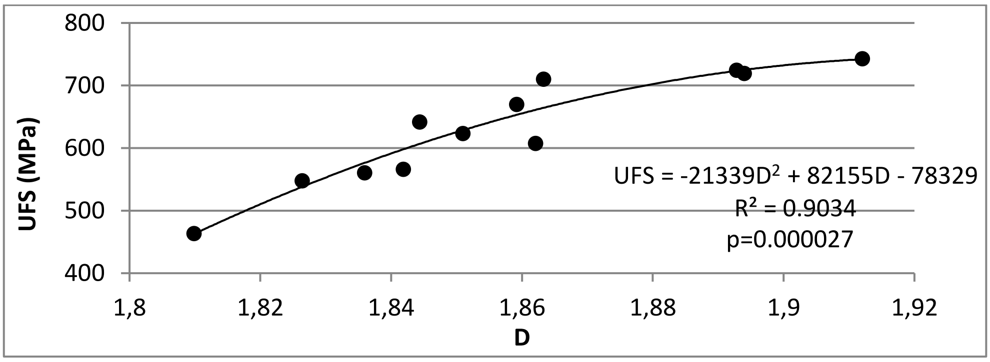

Figure 2: Ultimate flexural strength (UFS) versus fractal dimension D.

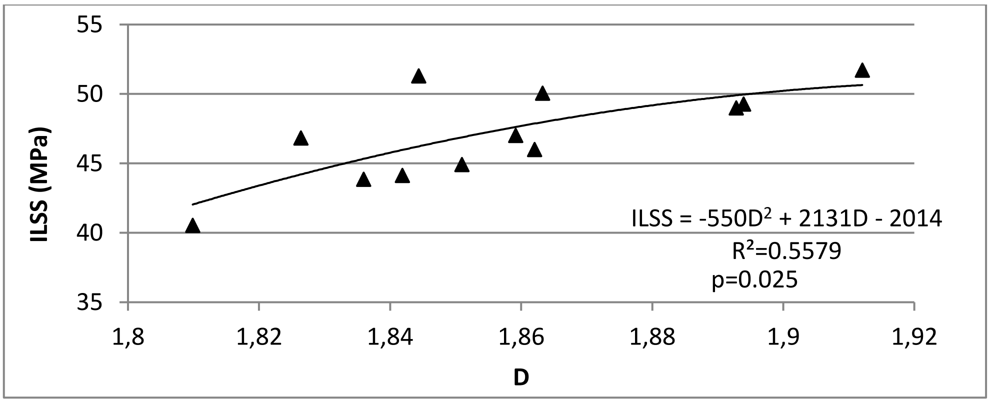

Figure 3: Interlaminar shear strength (ILSS) versus fractal dimension D.

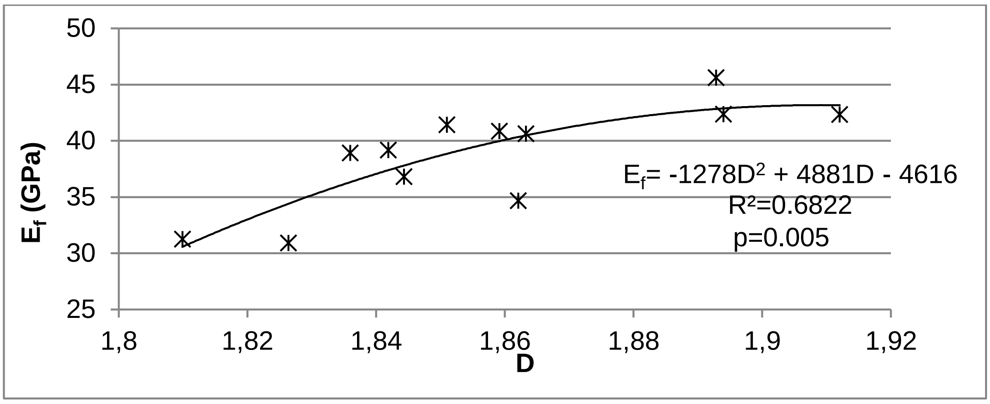

Figure 4: Flexural modulus of elasticity (E_f) versus fractal dimension D.

Figures 5-7 present the S-N fatigue data for specimens with 4, 5 and 6 layers of fabric. Figure 5 demonstrates that the T4wt laminate shows a high fatigue strength deriving from its high UFS and high D, while the P4wt laminate shows a lower fatigue strength due to its low UFS and low D (see Table 1). Fatigue life ranks in the sequence T4wt >P4wp >T4wp > P4wt, i.e. when the laminates are subjected to the same flexural stress, it is expected that, on average. This observation can be related to the static properties, where $UFS_{T4wt} > UFS_{P4wp} > UFS_{T4wp} > UFS_{P4wt}$. Furthermore, the ranking is the same for the fibre distribution, which is measured by the D, where $D_{T4wt} > D_{P4wp} > D_{T4wp} > D_{P4wt}$ as shown in Table 1. Similar behaviour is observed, for the same reasons, with the five and six fabric layer laminates, as shown in Figures 6 and 7 respectively. These observations lead to the conclusion that in these laminates, the fatigue life depends on the fibre distribution (as characterised by the D) and that laminates with high flexural strength will show high fatigue life, as has been observed by other workers [56]. This leads to general hypothesis that fatigue life is proportional to the D and to the UFS.

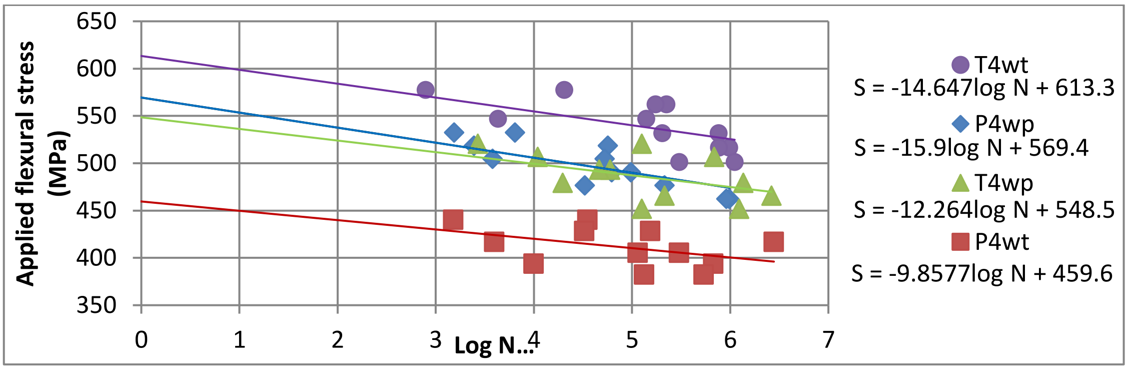

Figure 5: S-N curves for 4 layer plain and twill weave laminates in both the warp and weft directions.

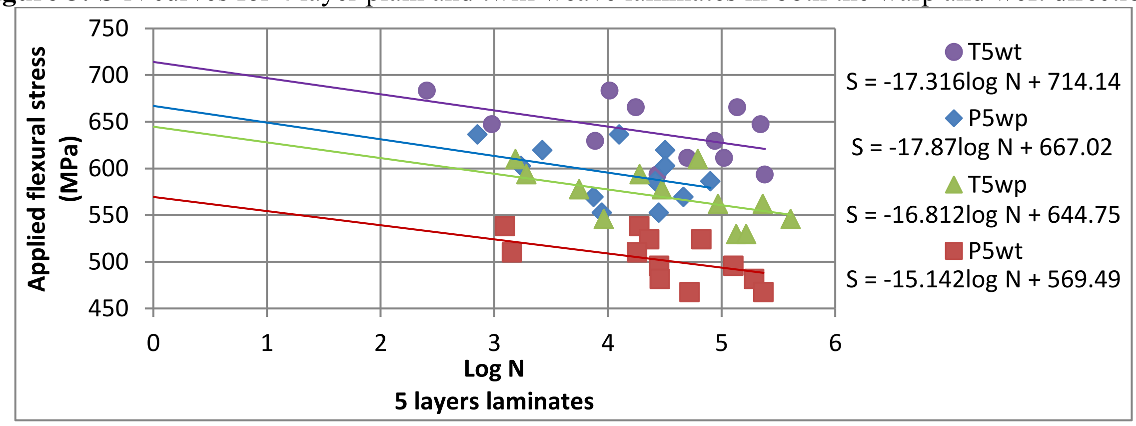

Figure 6: S-N curves for 5 layer plain and twill weave laminates in both the warp and weft directions.

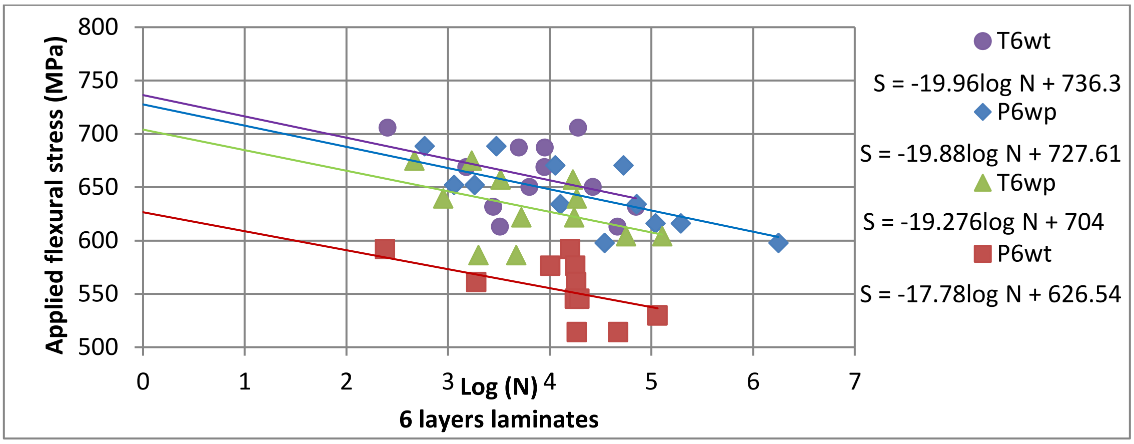

Figure 7: S-N curves for 6 layer plain and twill weave laminates in both the warp and weft directions.

The applied fatigue loads were recorded automatically by the Electropuls testing machine, allowing the actual flexural modulus, E_{ff}, to be calculated at any point in the fatigue test. Figure 8 presents normalised flexural modulus data, i.e. the ratio of E_{ff} to the original flexural modulus, E_o, as a function of life fraction, N/N_f, for all five layer laminates at an applied load of 85%UFS. As expected, it demonstrates that the change in flexural modulus can be divided into three regions, and that the data for all the 5-layer laminate types except for the plain weave fabric in the warp direction, group into a single scatter band of data. This particular case shows a higher value of E_{ff}/E_o for approximately the first 60% of the fatigue life than observed with the other laminate types.

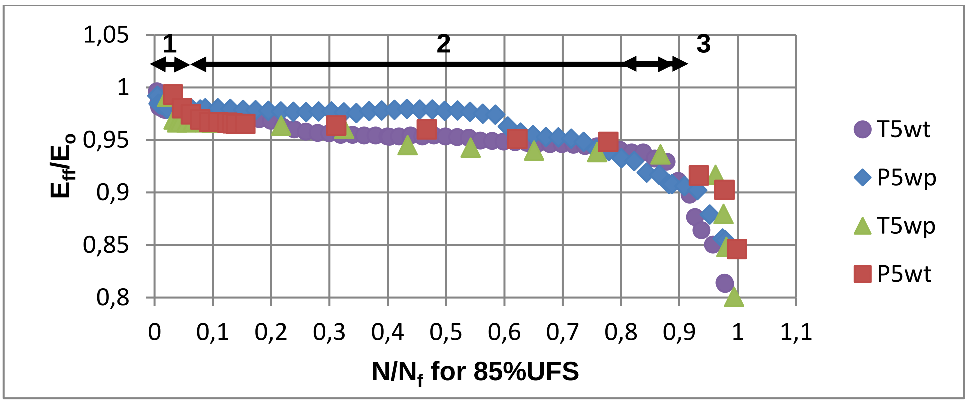

Figure 8: Normalised flexural modulus as a function of fatigue life fraction for the 5-layer laminates tested at 85% of the UFS.

In the specimens tested in this research, a 5-6% decrease in the flexural modulus indicates the beginning of the region of final failure in the composite laminates under fatigue loading. This decrease could be related to the rise of temperature that usually accompanies increasing deformation during fatigue testing [54]. It was observed that most of the fatigue specimens failed in the expected central region (middle of the inner loading roller span). However, some specimens failed near to one of the loading points, particularly at higher applied load levels, i.e. 90-95%UFS. In these cases cracking did not begin exactly below the loading point, but rather in close proximity to it. This could be due to the local stress concentration becoming more important at higher applied loads, as a result of the compression stresses induced at the loading point (leading to a localised multiaxial stress state) as well as a potential thermal influence from friction and fretting between the loading point and the specimen

5. Conclusions

The following conclusions can be drawn from the work reported in this study:

a. Fibre distribution, characterised by the fractal dimension (D), can be used as a parameter to characterise the static and fatigue properties of fibre-reinforced composites tested in four-point bend.

b. The corollary to this conclusion is that the ultimate flexural strength (UFS) of the composite laminates shows a clear dependence on the fibre distribution.

c. Interlaminar shear strength, ILSS, can also be correlated with the fibre distribution of the composite laminates, although the correlation is less significant than that identified for the UFS.

d. In these composite specimens, a decrease of 5-6 % in their flexural modulus indicates the occurrence of damage zones in the plates and the onset of fatigue failure. This occurs at about 90% of the fatigue life at a particular stress level.

References

[1] Holmes, M., Global carbon fibre market remains on upward trend. *Reinforced Plastics*, 2014. 58(6): p. 38-45.

[2] Toll, S. and J.A.E. Manson, Elastic Compression of a Fiber Network. *Journal of Applied Mechanics*, 1995. 62(1): p. 223-226.

[3] Toll, S. and J.-A. Månson. An analysis of the compressibility of fibre assemblies. in *6th Int. Conf. Fibre Reinf. Compos*. 1994.

[4] Pearce, N. and J. Summerscales, The compressibility of a reinforcement fabric. *Composites Manufacturing*, 1995. 6(1): p. 15-21.

[5] Toll, S., Packing mechanics of fiber reinforcements. *Polymer Engineering & Science*, 1998. 38(8): p. 1337-1350.

[6] Abraham, D., S. Matthews, and R. McIlhagger, A comparison of physical properties of glass fibre epoxy composites produced by wet lay-up with autoclave consolidation and resin transfer moulding. *Composites Part A: Applied Science and Manufacturing*, 1998. 29(7): p. 795-801.

[7] Botelho, E., et al., Evaluation of fatigue behavior on repaired carbon fiber/epoxy composites. *Journal of Materials Science*, 2008. 43(9): p. 3166-3172.

[8] Worrall, C. and G. Wells. Fiber distribution in discontinuous fiber reinforced plastics: characterization and effect of material performance. in ECCM-7: *Seventh European Conference on Composite Materials. Realising Their Commercial Potential*. 1996.

[9] Pearce, N.R.L., F.J. Guild, and J. Summerscales, An investigation into the effects of fabric architecture on the processing and properties of fibre reinforced composites produced by resin transfer moulding. *Composites Part A: Applied Science and Manufacturing*, 1998. 29(1-2): p. 19-27.

[10] Pearce, N.R.L., J. Summerscales, and F.J. Guild, Improving the resin transfer moulding process for fabric-reinforced composites by modification of the fabric architecture. *Composites Part A: Applied Science and Manufacturing*, 2000. 31(12): p. 1433-1441.

[11] Summerscales, J., et al., Voronoi cells, fractal dimensions and fibre composites. *Journal of Microscopy*, 2001. 201(2): p. 153-162.

[12] Summerscales, J., et al., The fractal dimension of X-ray tomographic sections of a woven composite. *Advanced composites letters*, 2004. 13(2): p. 113-121.

[13] Picu, R., et al., Composites with fractal microstructure: The effect of long range correlations on elastic–plastic and damping behavior. Mechanics of Materials, 2014. 69(1): p. 251-261.

[14] Gao, S.-L., E. Mäder, and S.F. Zhandarov, Carbon fibers and composites with epoxy resins: Topography, fractography and interphases. *Carbon*, 2004. 42(3): p. 515-529.

[15] Allen, M., G.J. Brown, and N.J. Miles, Measurement of boundary fractal dimensions: review of current techniques. *Powder Technology*, 1995. 84(1): p. 1-14.

[16] Celli, A., et al., Fractal analysis of cracks in alumina–zirconia composites. *Journal of the European Ceramic Society*, 2003. 23(3): p. 469-479.

[17] Biancolini, M.E., et al., Fatigue cracks nucleation on steel, acoustic emission and fractal analysis. *International Journal of Fatigue*, 2006. 28(12): p. 1820-1825.
[18] Kuznetsov, P.V., V.E. Panin, and J. Schreiber, Fractal dimension as a characteristic of deformation stages of austenite stainless steel under tensile load. *Theoretical and Applied Fracture Mechanics*, 2001. 35(2): p. 171-177.
[19] Venkatesh, B., D.L. Chen, and S.D. Bhole, Three-dimensional fractal analysis of fracture surfaces in a titanium alloy for biomedical applications. *Scripta materialia*, 2008. 59(4): p. 391-394.
[20] Wang, L., L.-d. Wang, and W.-d. Fei, Fractal analysis of fracture surfaces in aluminum borate whisker-reinforced aluminum alloy 6061 composite. *Transactions of Nonferrous Metals Society of China*, 2011. 21(3): p. 461-466.
[21] Yuan, C.Q., et al., The use of the fractal description to characterize engineering surfaces and wear particles. *Wear*, 2003. 255(1–6): p. 315-326.
[22] Mishnaevsky, L., Hierarchical composites: Analysis of damage evolution based on fiber bundle model. *Composites Science and Technology*, 2011. 71(4): p. 450-460.
[23] Aniszewska, D. and M. Rybaczuk, Fractal characteristics of defects evolution in parallel fibre reinforced composite in quasi-static process of fracture. *Theoretical and Applied Fracture Mechanics*, 2009. 52(2): p. 91-95.
[24] Campos, K.A.d., et al., 3-D reconstruction by extended depth-of-field in failure analysis – Case study II: Fractal analysis of interlaminar fracture in carbon/epoxy composites. *Engineering Failure Analysis*, 2012. 25(0): p. 271-279.
[25] Pimenta, S. and S.T. Pinho, An analytical model for the translaminar fracture toughness of fibre composites with stochastic quasi-fractal fracture surfaces. *Journal of the Mechanics and Physics of Solids*, 2014. 66: p. 78-102.
[26] Mishnaevsky Jr, L., Hierarchical composites: Analysis of damage evolution based on fiber bundle model. *Composites Science and Technology*, 2011. 71(4): p. 450-460.
[27] Foroutan-Pour, K., P. Dutilleul, and D. Smith, Advances in the implementation of the box-counting method of fractal dimension estimation. *Applied Mathematics and Computation*, 1999. 105(2): p. 195-210.
[28] Pitchumani, R. and B. Ramakrishnan, A fractal geometry model for evaluating permeabilities of porous preforms used in liquid composite molding. *International journal of heat and mass transfer*, 1999. 42(12): p. 2219-2232.
[29] Buczkowski, S., P. Hildgen, and L. Cartilier, Measurements of fractal dimension by box-counting: a critical analysis of data scatter. *Physica A: Statistical Mechanics and its Applications*, 1998. 252(1–2): p. 23-34.
[30] Li, J., Q. Du, and C. Sun, An improved box-counting method for image fractal dimension estimation. *Pattern Recognition*, 2009. 42(11): p. 2460-2469.
[31] Buczkowski, S., et al., The modified box-counting method: analysis of some characteristic parameters. *Pattern Recognition*, 1998. 31(4): p. 411-418.
[32] Chen, S.S., J.M. Keller, and R.M. Crownover, On the calculation of fractal features from images. Pattern Analysis and Machine Intelligence, *IEEE Transactions* on, 1993. 15(10): p. 1087-1090.
[33] Jin, X. and S. Ong. Scale limits in estimating fractal dimensions of image surfaces. in Networks, 1993. International Conference on Information Engineering'93.'Communications and Networks for the Year 2000', *Proceedings of IEEE Singapore International Conference* on. 1993. IEEE.
[34] Basford, D.M., et al., Relationship between mechanical performance and microstructure in composites fabricated with flow-enhancing fabrics. Composites, 1995. 26(9): p. 675-679.
[35] Hale, R.D., An experimental investigation into strain distribution in 2D and 3D textile composites. *Composites Science and Technology*, 2003. 63(15): p. 2171-2185.

[36] Aziz, S.H. and M.P. Ansell, The effect of alkalization and fibre alignment on the mechanical and thermal properties of kenaf and hemp bast fibre composites: Part 1 – polyester resin matrix. Composites Science and Technology, 2004. 64(9): p. 1219-1230.
[37] Gojny, F.H., et al., Influence of nano-modification on the mechanical and electrical properties of conventional fibre-reinforced composites. *Composites Part A: Applied Science and Manufacturing*, 2005. 36(11): p. 1525-1535.
[38] Tzetzis, D. and P.J. Hogg, Bondline toughening of vacuum infused composite repairs. *Composites Part A: Applied Science and Manufacturing*, 2006. 37(9): p. 1239-1251.
[39] Dhakal, H.N., Z.Y. Zhang, and M.O.W. Richardson, Effect of water absorption on the mechanical properties of hemp fibre reinforced unsaturated polyester composites. *Composites Science and Technology*, 2007. 67(7–8): p. 1674-1683.
[40] Lomov, S.V., et al., Full-field strain measurements for validation of meso-FE analysis of textile composites. *Composites Part A: Applied Science and Manufacturing*, 2008. 39(8): p. 1218-1231.
[41] Sudarisman and I.J. Davies, The effect of processing parameters on the flexural properties of unidirectional carbon fibre-reinforced polymer (CFRP) composites. *Materials Science and Engineering*: A, 2008. 498(1-2): p. 65-68.
[42] Colin de Verdiere, M., et al., Evaluation of the mechanical and damage behaviour of tufted non crimped fabric composites using full field measurements. *Composites Science and Technology*, 2009. 69(2): p. 131-138.
[43] Liu, R.-m. and D.-k. Liang, Experimental study of carbon fiber reinforced plastic with embedded optical fibers. *Materials & Design*, 2010. 31(2): p. 994-998.
[44] Heß, H. and N. Himmel, Structurally stitched NCF CFRP laminates. Part 2: Finite element unit cell based prediction of in-plane strength. *Composites Science and Technology*, 2011. 71(5): p. 569-585.
[45] Vaughan, T.J. and C.T. McCarthy, A micromechanical study on the effect of intra-ply properties on transverse shear fracture in fibre reinforced composites. *Composites Part A: Applied Science and Manufacturing*, 2011. 42(9): p. 1217-1228.
[46] Demers, C.E., Tension–tension axial fatigue of E-glass fiber-reinforced polymeric composites: fatigue life diagram. Construction and Building Materials, 1998. 12(5): p. 303-310.
[47] Kalam, A., et al., Fatigue behaviour of oil palm fruit bunch fibre/epoxy and carbon fibre/epoxy composites. *Composite Structures*, 2005. 71(1): p. 34-44.
[48] Kawai, M., et al., High-temperature off-axis fatigue behaviour of unidirectional carbon-fibre-reinforced composites with different resin matrices. *Composites Science and Technology*, 2001. 61(9): p. 1285-1302.
[49] Aymerich, F., P. Priolo, and C.T. Sun, Static and fatigue behaviour of stitched graphite/epoxy composite laminates. *Composites Science and Technology*, 2003. 63(6): p. 907-917.
[50] Chambers, A.R., et al., The effect of voids on the flexural fatigue performance of unidirectional carbon fibre composites developed for wind turbine applications. *International Journal of Fatigue*, 2006. 28(10): p. 1389-1398.
[51] Ferreira, J.A.M., et al., Analysis of fatigue and damage in glass-fibre-reinforced polypropylene composite materials. *Composites Science and Technology*, 1999. 59(10): p. 1461-1467.
[52] Bertin, M., F. Touchard, and M.-C. Lafarie-Frenot, Experimental study of the stacking sequence effect on polymer/composite multi-layers submitted to thermomechanical cyclic loadings. *International Journal of Hydrogen Energy*, 2010. 35(20): p. 11397-11404.
[53] De Monte, M., E. Moosbrugger, and M. Quaresimin, Influence of temperature and thickness on the off-axis behaviour of short glass fibre reinforced polyamide 6.6 – cyclic loading. *Composites Part A: Applied Science and Manufacturing*, 2010. 41(10): p. 1368-1379.
[54] Ferreira, J.A.M., J.D.M. Costa, and P.N.B. Reis, Static and fatigue behaviour of glass-fibre-reinforced polypropylene composites. *Theoretical and Applied Fracture Mechanics*, 1999. 31(1): p. 67-74.

[55] Fuqiang, W. and Y. Weixing, A Model of the Fatigue Life Distribution of Composite Laminates Based on Their Static Strength Distribution. *Chinese Journal of Aeronautics*, 2008. 21(3): p. 241-246.
[56] Caprino, G. and A. D'Amore, Flexural fatigue behaviour of random continuous-fibre-reinforced thermoplastic composites. *Composites Science and Technology*, 1998. 58(6): p. 957-965.
[57] Epaarachchi, J.A., Effects of static–fatigue (tension) on the tension–tension fatigue life of glass fibre reinforced plastic composites. *Composite Structures*, 2006. 74(4): p. 419-425.
[58] Epaarachchi, J.A. and P.D. Clausen, An empirical model for fatigue behavior prediction of glass fibre-reinforced plastic composites for various stress ratios and test frequencies. *Composites Part A: Applied Science and Manufacturing*, 2003. 34(4): p. 313-326.
[59] Quaresimin, M., L. Susmel, and R. Talreja, Fatigue behaviour and life assessment of composite laminates under multiaxial loadings. *International Journal of Fatigue*, 2010. 32(1): p. 2-16.
[60] Flore, D. and K. Wegener, Modelling the mean stress effect on fatigue life of fibre reinforced plastics. *International Journal of Fatigue*, 2016. 82, Part 3: p. 689-699.